

Received: 2015.12.22  
Accepted: 2016.02.05  
Published: 2016.10.19

# Altered microRNA-9 Expression Level is Directly Correlated with Pathogenesis of Nonalcoholic Fatty Liver Disease by Targeting *Onecut2* and *SIRT1*

Authors' Contribution:  
Study Design A  
Data Collection B  
Statistical Analysis C  
Data Interpretation D  
Manuscript Preparation E  
Literature Search F  
Funds Collection G

ABCDEF **Ran Ao**  
BCDE **Ying Wang**  
BCDF **Jing Tong**  
DEF **Bai-Fang Wang**

Department of Gastroenterology, The First Affiliated Hospital of China Medical University, Shenyang, Liaoning, P. R. China

**Corresponding Author:** Ran Ao, e-mail: aoranar0722@163.com

**Source of support:** This study was funded by the Scientific Research of the First Hospital of China Medical University (fsfh1313); Tianqing Liver Disease Research Foundation, Chinese Foundation for Hepatitis and Prevention and Control (20120101)

**Background:** MicroRNA-9 (miR-9) was detected in nonalcoholic fatty liver disease (NAFLD) patients to understand the role of miR-9 in NAFLD development.


**Material/Methods:** Between February 2014 and February 2015, 105 cases of NAFLD were recruited and confirmed by liver biopsy pathology, including patients with mild NAFLD (n=58) and moderate-severe NAFLD (n=47); nonalcoholic steatohepatitis (NASH) (n=53) and non-NASH (n=52); and 50 healthy participants were regarded as the healthy control group. MiR-9 expression was measured by qRT-PCR. For *in vitro* experiments, L-02 normal liver cells were divided into normal control group (cultured with original culture medium), dimethyl sulfoxide (DMSO) group (cultured with DMSO) and oleic acid group (cultured with oleic acid to induce fatty change), and MTT assay was used to measure the effect of different oleic acid concentrations on cell proliferation. Nile red staining was used to detect intracellular accumulation of lipid droplets. Further, synthetic miR-9 mimic and its control and miR-9 inhibitors and its control were independently transfected into L-02 cells.

**Results:** MiR-9 levels in the mild NAFLD group and moderate-severe NAFLD group were significantly higher than in the healthy control group (both  $P < 0.05$ ). Mean fluorescence intensity of lipid droplets increased with the duration of induction, and were dramatically higher in oleate-treated L-02 cells; intracellular triglyceride (TG) content was also higher. miR-9 levels significantly increased following oleate induction. Importantly, miR-9 levels were significantly elevated upon miR-9 mimic transfection. Conversely, miR-9 level was lowered with miR-9 inhibitors transfection. Additionally, *Onecut2* and *SIRT1* were identified as miR-9 targets.

**Conclusions:** A positive relationship between miR-9 and steatosis was established with our results that miR-9 mimic transfection decreased intracellular lipid content. Finally, we identified 2 miR-9 targets, *Onecut2* and *SIRT1*, which may be crucial players in NAFLD development.

**MeSH Keywords:** **Fatty Liver • Oleic Acid • RNA Interference**

**Full-text PDF:** <http://www.medscimonit.com/abstract/index/idArt/897207>

 5284

 6

 8

 45



## Background

Fatty liver diseases are classified into alcoholic liver disease (ALD) related to heavy alcohol drinking, and nonalcoholic fatty liver disease (NAFLD) characterized by fat accumulation in the liver in the absence of alcohol intake [1]. As the most common form of chronic liver disease, 30% of the population in developed countries is affected by NAFLD [2,3]. NAFLD may progress through multiple mechanisms, including increased hepatic TAG synthesis, elevated hepatic uptake of free fatty acids, and impaired  $\beta$ -oxidation or transport of free fatty acids from the liver [4,5]. Additionally, obesity, metabolic syndromes, insulin resistance, hyperinsulinemia, systolic hypertension, and dyslipidemia are very closely associated with NAFLD development and progression [6]. The NAFLD disease spectrum ranges from steatosis to steatohepatitis (NASH), and is a complex disease influenced by both environmental and genetic factors, with multiple independent disease modifiers that control NAFLD pathogenesis and progression [7–9]. Potential therapeutic targets for NAFLD are in urgent need and, in this context, microRNAs have recently gained significant attention for their crucial cellular roles in regulating pathways that are highly relevant to human diseases [10,11].

MicroRNAs (miRNAs) are small endogenous non-coding RNAs of 19–25 nucleotides in length and are key regulators of post-transcriptional gene expression [12,13]. Abnormal expression of miRNAs is associated with several human diseases such as cancer, diabetes, metabolic disorders, neurological disorders, and cardiovascular diseases. For this reason, microRNAs are important both as biomarkers and as therapeutic targets for clinical applications in several human pathological states [14]. Indeed, Yue Zhao et al. found significantly elevated expression levels of miR-30c, miR-338, miR-34a, and Let-g, and reduced levels of miR-148b and miR-9 expression in HepG2 hepatocellular carcinoma cell line compared to normal liver cell line L-02 [15]. Interestingly, Ramachandran et al. reported that miR-9 plays similar roles during glucose-dependent secretion in pancreatic  $\beta$ -islets by targeting Sirt1. They found reduced Sirt1 levels when miR-9 expression was high and proposed that the functional link between miR-9 and Sirt1 expression levels could be relevant to diabetes [16]. Recent evidence also suggests that abnormal expression of miRNAs interfere with insulin-mediated signal transduction, resulting in insulin resistance, and abnormal lipid metabolism, and eventually promotes NAFLD development. However, current research in miRNA and NAFLD is still in its early stages and there is no firm consensus on the underlying mechanisms and targetable miRNAs for NAFLD treatment [17]. It is also not entirely clear if miR-9 functions in specific pathways or is more broadly involved in cellular mechanisms since Miranda et al. reported the value of several miRNAs, including miR-9, as therapeutic targets for alcohol-related disorders [18]. Surprisingly, despite the close

association between metabolic disorders and NAFLD, there is no study yet reporting the potential relationship between miR-9 and NAFLD. In this study, we examined the miR-9 expression levels in NAFLD to understand the prognostic and therapeutic value of miR-9 in NAFLD development.

## Material and Methods

### Subjects

A total of 155 study participants underwent health examinations at the medical center of the First Affiliated Hospital of China Medical University between February 2014 and February 2015. Among them, 105 cases of NAFLD were confirmed by B ultrasonic diagnosis and liver biopsy pathology, including patients with mild NAFLD (n=58) and moderate-severe NAFLD (n=47); nonalcoholic steatohepatitis (NASH) (n=53) and non-NASH (n=52); and 50 healthy participants with normal liver enzymes and abdominal ultrasonography findings were regarded as the healthy control group. The inclusion criteria were: (1) 18 years or older; (2) persistently elevated aminotransferases for at least 6 months; (3) hyperechogenic liver diagnosed by ultrasonography; and (4) liver histology with a diagnosis of NASH without cirrhosis obtained no more than 6 months before the study. The exclusion criteria were: (1) alcohol consumption history; (2) hypertension; (3) any other form of chronic liver disease; (4) use of any medications which might cause or affect NAFLD; (5) abnormal thyroid function tests; (6) fasting plasma glucose (FPG) more than 126 mg/dL or anti-diabetic drug use; (7) chronic obstructive pulmonary disease; peripheral and cerebral vascular disease; hematologic disorders; acute or chronic infection; cancer history of cancer; and chronic kidney diseases. All subjects underwent a clinical examination and were questioned regarding their medical history. This study was approved by the Ethics Committee of the First Affiliated Hospital of China Medical University and informed consent was obtained from all human subjects. The ethics approval for this study conformed to the standards of the Declaration of Helsinki [19].

### B ultrasound diagnostic criteria

B ultrasound diagnostic criteria of NAFLD were based on the NAFLD imaging diagnostic criteria published by Chinese Medical Association in 2006 [20]: (1) diffuse enhanced liver near-field echo (stronger than that in the kidney and spleen) and gradually attenuated far-field echo; (2) unclear intrahepatic duct structure; (3) mild to moderate enlargement of liver with round and blunt edge angle; (4) color Doppler flow imaging showed reduced or no flow signals in the liver but normal liver blood vessels direction; and (5) unclear or incomplete liver right lobe capsule and diaphragm echoes. Mild NAFLD patients were

**Table 1.** Real-time fluorescence quantitative PCR (qRT-PCR) primer sequences.

Sequences	
U6	RT primer: 5'CGCTTCACGAATTTGCGTGCAT3'
	PCR primers: F: 5'GCTTCGGCAGCACATATACTAAAAT3' R: 5'CGCTTCACGAATTTGCGTGCAT3'
	RT primer: 5'GTCGTATCCAGTGCCTGTCGTGGAGTCGGCAATTCAGTGGATACGACTCATAACA3'
MiR-9	PCR primers: GSP: 5'GGGGGTCTTTGGTTATCTA3' R: 5'CAGTGCCTGTCGTGGA3'

RT – real-time; PCR – polymerase chain reaction; F – forward primer; R – reverse primer; GSP – gene specific prime.

diagnosed with (1) and one of (2) to (4); moderate NAFLD patients were diagnosed with (1) and two of (2) to (4); and severe NAFLD patients were diagnosed with (1), two of (2) to (4), and (5). Computer tomography (CT) criteria were: generally lowered liver density, mild NAFLD patients were diagnosed with liver/spleen CT value more than 0.7 and less than 10, moderate NAFLD patients with liver/spleen CT value more than 0.5 and less than 0.7, and severe NAFLD patients with liver/spleen CT value less than 0.5. All the fatty livers were uniform fatty liver, and were jointly confirmed by 2 attending physicians.

### Pathological diagnosis

We used the guidelines for NAFLD activity score (NAS) published by NASH Clinical Research Network pathology working group of the US National Institutes of Health and liver fibrosis staging [21]. NAS (0–8 points): (1) hepatic steatosis: 0 point (<5%); 1 point (5% to 33%); 2 points (34% to 66%); and 3 points (>66%); (2) lobular inflammation (necrosis detected by 20 times of microscope counting): 0 point, none; 1 point (<2); 2 points (2 to 4); and 3 points (>4); (3) hepatocyte ballooning degeneration: 0 point, none; 1 point, rare; and 2 points, common. NAS is a semi-quantitative scoring system; patients with NAS less than 3 points can be excluded from NASH, while patients with NAS more than 4 points can be diagnosed as NASH, and patients with NAS between 3 to 4 points can be regarded as possible NASH. Liver fibrosis stages (0–4) are: 0: no fibrosis; 1a: mild perisinusoidal fibrosis in the hepatic acinar zone 3; 1b: moderate perisinusoidal fibrosis in the hepatic acinar zone 3; 1c: only portal perivascular fibrosis; 2: combined perisinusoidal fibrosis in the hepatic acinar zone 3 and portal perivascular fibrosis; 3: bridging fibrosis; and 4: highly suspected or confirmed cirrhosis, including combined NASH with cirrhosis, fatty liver cirrhosis and cryptogenic cirrhosis (liver steatosis and inflammation are alleviated with the progression of liver fibrosis). NASH was diagnosed with liver fibrosis stage more than 2 [22].

### General information

Medical history was recorded and fasting height, weight, waist circumference, hip circumference, and systolic and diastolic blood pressure were measured. Body mass index (BMI=weight/height<sup>2</sup>) and waist-hip ratio (WHR=waist circumference/hip circumference) were calculated.

### Conventional biochemical indices

Fasting elbow venous blood (8 ml) of each study participants was collected. Three ml of the blood samples without anticoagulation was placed in a water bath at 37°C for 30 min and centrifuged at 1400×g, the supernatant was collected and kept at –20°C for the measurement of the following liver function indices: alanine aminotransferase (ALT), aspartate aminotransferase (AST), gamma-glutamyl transferase (GGT) and total bile acid (TBA), total cholesterol (TC), triglyceride (TG), low-density lipoprotein cholesterol (LDL-C), high-density lipoprotein cholesterol (HDL-C), and fasting plasma glucose (FPG), using a HITACHI 7060 automatic biochemical analyzer (Hitachi 7060, Hitachi Ltd., Tokyo, Japan). The other 5 ml of blood samples were centrifuged at 1200×g for 10 min at 4°C; then, the upper fluid was transferred to a 1.5-ml Eppendorf tube and centrifuged at 12 000×g for 10 min at 4°C. Subsequently, the supernatant was carefully moved into a new Eppendorf tube and stored at –70°C for the detection of miR-9 expression.

### Real-time fluorescence quantitative PCR (qRT-PCR) for miR-9 expression

Total RNA was extracted from blood samples (5 ml) using Trizol reagent (Invitrogen, USA). The concentration of purified RNA was determined by measuring the absorbance at OD260/OD280. RNA purity was excellent and in the range of 1.9–2.1. RNA integrity was confirmed by agarose gel electrophoresis. The total RNA was used for synthesis of first-strand cDNA

with an mRNA reverse transcription Kit (EXIQON). Relative expression level of miR-9 was measured by qRT-PCR as previously described [23]. The primer sequences are shown in Table 1. An MJ-research fluorescence quantitative PCR instrument was used for qRT-PCR and the software operating system was opticon Monitor 2. The qRT-PCR reagent kit was purchased from Exiqon (Vedbaek, Denmark). The reaction conditions were: pre-denaturing for 5 min at 95°C, followed by 10 s at 95°C, and 1 min at 60°C, for 40 cycles in total. U6 was used as internal control and the relative expression of miRNA was analyzed by 2- $\Delta\Delta$ CT method.

### Cell culture and experimental groups

Immortal normal human hepatic cell line L-02 was purchased from the Sun Yat-sen University cell bank. Cells were cultured in RPMI-1640 complete medium (USA GIBCO company) containing 10% fetal bovine serum (FBS) as previously described [24] and incubated at 5% CO<sub>2</sub> and 37°C. Growth medium was changed every 3 days. Cells were distributed into 3 groups after 24-h growth: normal group, dimethyl sulfoxide (DMSO) group, and oleic acid group. The cells were cultured further in fresh culture medium. The normal group contained culture medium with no additions, the DMSO group contained culture medium with different concentrations of DMSO (GIBCO, USA) (0.00%, 0.01%, 0.02%, 0.04%, 0.08%, and 1.60%), and the oleic acid group contained culture medium with different concentrations of oleic acid dissolved in DMSO (Sigma, USA) (5 g/ml, 10 g/ml, 20 g/ml, and 40 g/ml). The oleic acid concentrations were adjusted to ensure that the final concentrations of DMSO in both the DMSO group and the oleic acid group were the same.

### Determination of optimal concentration of oleic acid by MTT assay

Excess oleic acid overloading triggers apoptosis. Thus, optimal oleate concentration was determined to avoid triggering apoptosis and to maintain healthy cell growth. Optimal concentration of oleic acid was determined using MTT assay as previously reported [25]. L-02 cells from each group were inoculated in 96-well culture plates at 104 cells per well. Culture medium was set for the zero well. Five parallel wells were set for each group and cells were incubated for 24 h at 37°C with 5% CO<sub>2</sub>. Oleic acid induction in L-02 cells and subsequent steps for MTT assay were based on a previously published protocol [26]. A volume of 20  $\mu$ l MTT solution (Sigma, USA) was added to each well at 24 h, 48 h, and 72 h, and the cells were further incubated for 4 h. Next, culture medium was carefully aspirated and 150  $\mu$ l DMSO solution was added to each well and mixed well for 10 min on a micro-plate oscillator to dissolve formazan crystals. The absorbance was measured at OD490 nm using an ELISA plate reader.

### Lipid droplet detection with Nile red staining

Formation of lipid droplet in normal and oleate-induced cells was monitored using standard Nile red staining conditions as previously described [27]. Cells were grown on 2.4×2.4 cm cover glasses in 6-well plates in 2.5 ml cell culture medium. Following the determination of optimal oleate concentrations, oleic acid was added to each well at a final concentration of 20  $\mu$ g/ml. Cells were cultured for an additional 24 h, 48 h, or 72 h. At the end of these time points, cover glasses were removed, washed 4–5 times with PBS and fixed with paraformaldehyde for 10 min. Diluted and filtered Nile red solution (1–2 ml, Sigma, USA) was added to the cover glasses and stained for 10 min at room temperature. Nile red solution was removed and, after washing 3–5 times with PBS, the cover glass was mounted on a glass slide and sealed. Confocal images were acquired using a laser scanning confocal microscope (Olympus, Japan). A total of 10 high-power fields (HPFs) were randomly selected and 3 cells per each HPF were randomly chosen for fluorescence intensity analysis using Olympus Fluview ver. 3 viewer software.

### Determination of intracellular TG content in L-02 cells

Cells were seeded separately into 6-well plates as the normal control group (DMSO added) and oleic acid-induced group (induced with oleic acid in DMSO). Oleate induction was for 24 h, 48 h, or 72 h. Next, cells were collected at the end of each time point and 5–10×10<sup>6</sup> cells were resuspended in 1 ml of PBS. Cell lysis was performed with an ultrasonicator (200 W, 3×3s) and the cleared supernatant was collected for subsequent measurements. The intracellular TG content was measured at OD570 by colorimetry method using the TG Kit (Biovision, CA, USA) as previously reported [25]. TG content was calculated as: C=TS/SV nmol/ $\mu$ l, TS is the content of TG in standard curve (nmol), and SV is the sample volume added in the sample well (before dilution) ( $\mu$ l).

### Cells transfection

Transient transfections were performed using LipofectamineTM2000 (Invitrogen, USA). One day before transfection, cells were plated in 6-well plates containing 2.5 ml RPMI-1640 culture medium and incubated overnight at 37°C with 5% CO<sub>2</sub>. Next, cells were transfected at 30–50% confluency. Steatotic cells induced by oleic acid (20  $\mu$ g/ml) were divided into: the miR-9 mimic group (transfected with miR-9 mimics), the miR-9 mimic negative control (NC) group (transfected with miR-9 mimic NC), the miR-9 inhibitor group (transfected with miR-9 inhibitors), the miR-9 inhibitor NC group (transfected with miR-9 inhibitor NC), the non-transfected steatotic cell group (non-transfection), and the normal control (NC) group. The miR-9 mimics and inhibitors were purchased from Dharmacon

(Dharmacon RNA Technologies, Lafayette, CO, USA). miRNA/Lipofectamine-2000 was dripped into 6-well plates, and 72 h later total RNA was isolated and miR-9 expression levels were measured by qRT-PCR. Lipid droplet formation was observed by Nile red staining.

#### qRT-PCR for detection of miR-9 target gene expression

Total RNA was purified, as described above from the miR-9 mimic group, the mimic NC group, the miR-9 inhibitor group, the inhibitor NC group, and the untransfected cells group. The extracted RNA from each sample was reverse-transcribed into cDNA using a reverse transcription kit (Fermentas, UK). GAPDH, Onecut2, SIRT1, REST, and CoREST primers were used for qRT-PCR. The reaction conditions were as described above. Primer sequences were Onecut2: upstream primer: 5'-CATACTCAAGCGGGACCTCC-3', downstream primer: 5'-TTGGTGGAACTGGGAGTCTAA-3'; SIRT1: upstream primer: 5'-GAGTGGCAAAGGAGCAG-3', downstream primer: 5'-TCTGGCATGTCCCACTATC-3'; REST: upstream primer: 5'-GCAGCAAATGAGTCTCAGGA-3'; downstream primer: 5'-ACCAAATGGCGATTGAGGTG-3'; CoREST: upstream primer: 5'-TGAGCCTGAATCCTCCATTG-3', downstream primer: 5'-AGGCAGCCATTCCAGTCACA-3'.

#### Western blotting

Total protein was extracted by standard method as previously reported [28] and 50 µg total protein was resolved by 10% SDS-PAGE electrophoresis and transferred onto PVDF membranes. Following the transfer, the membrane was blocked for 1 h at room temperature with 5% skimmed milk. Subsequently, primary antibodies for Onecut2 (serial number: ab28466), SIRT1 (serial number: ab12193), REST (serial number: ab21635), and CoREST (serial number: ab32631) were added and incubated at 4°C overnight. Primary antibodies were purchased from Abcam (Cambridge, UK). The next day, secondary antibodies were added and incubated at 37°C for 1 h. Chemiluminescence-based detection was performed and results were imaged with a CCD camera.

#### Dual luciferase reporter gene assay

Target genes of miR-9 were analyzed using biological prediction site microRNA.org to verify if Onecut2, SIRT1, REST, and CoREST are direct target genes of miR-9. Full-length clone and amplification of 3' UTR region of the Onecut2, SIRT1, REST, and CoREST genes were carried out. The PCR products were cloned into the multiple cloning sites of pmirGLO (Promega) luciferase gene downstream, and site-specific mutagenesis were conducted on the binding sites for the bioinformatics prediction of miR-9 and target genes. pRL-TK vector (Takara) expressing Renilla luciferase was used as internal reference to adjust the

number of cells and the differences of transfection efficiency. miR-9 mimics and its NC were co-transfected with luciferase reporter vector into L-02 cells, and dual luciferase activity was measured by the method provided by Promega.

#### Statistical analysis

Data in each experimental group are expressed as mean ± standard deviation (SD) and analyzed by SPSS18.0 statistical software. The 2 independent-groups *t* test was used for comparisons of differences in miRNA expression levels in 2 groups that were normally distributed, with homogeneity of variance. The one-way analysis of variance (ANOVA) was used for comparisons between multiple groups. A non-parametric test was used to detect the differences in miRNA expression levels in groups that did not show normal distribution. The LSD *t* test was used for pair-wise comparisons. A value of  $P < 0.05$  was considered as statistically significant.

## Results

#### General information and biochemical parameters comparison

Basic information of the study subjects and the results of biochemical measurements in the study groups are shown in Tables 2 and 3. BMI, WHR, ALT, AST, GGT, TC, TG, LDL-C, and FPG in the mild NAFLD group and the moderate-severe NAFLD group were significantly higher compared with those in the healthy control group, while the liver/spleen CT value and HDL-C were obviously lower in the 2 NAFLD groups than those in the healthy control group (all  $P < 0.05$ ). The BMI, WHR, ALT, AST, GGT, TG, and FPG were also significantly higher, while the liver/spleen CT value was obviously decreased in the moderate-severe NAFLD group than those in the mild NAFLD group (all  $P < 0.05$ ). However, there were no significant differences in TC, LDL-C, and HDL-C between the mild NAFLD group and the moderate-severe NAFLD group (all  $P > 0.05$ ). BMI, WHR, ALT, AST, GGT, TC, TG, LDL-C, and FPG were significantly higher, while the liver/spleen CT value and HDL-C were lower in the non-NASH and NASH group compared with those in the healthy control group (all  $P < 0.05$ ). In comparison with the non-NASH group, ALT and GGT increased significantly while the liver/spleen CT value decreased obviously in the NASH group (all  $P < 0.05$ ).

#### Relative expression levels of miR-9 in each group

Relative expression levels of miR-9 were significantly different among the mild NAFLD group, moderate-severe NAFLD group, and the healthy control group ( $F = 299.4$ ,  $P < 0.001$ ). Compared with the healthy control group, the relative expression of miR-9 levels was obviously increased in the mild NAFLD group and

**Table 2.** General information and biochemical parameters comparison among the healthy control group and NAFLD groups.

	Healthy control group (n=50)	Mild NAFLD group (n=58)	Moderate-severe NAFLD group (n=47)	F/X2	P
Age (years)	47.26±7.56	45.5±6.4	46.3±9.9	0.367	0.694
Genders (M/F)	32/18	37/21	30/17	0.255	0.881
BMI	22.10±4.40	26.00±4.50*	28.80±5.10**	25.41	<0.001
WHR	0.80±0.30	1.10±0.30*	1.40±0.30**	48.47	<0.001
Liver/spleen CT value	1.33±0.08	0.86±0.09*	0.33±0.17**	750.8	<0.001
Systolic blood pressure (mmHg)	124.2±11.80	122.3±14.8	123.7±15.6	0.264	0.769
Diastolic blood pressure (mmHg)	83.50±6.20	82.20±7.60	83.10±6.70	0.507	0.603
ALT (U/L)	22.40±10.80	30.50±8.5*	101.70±17.10**	1162	<0.001
AST (U/L)	20.20±10.40	28.20±10.4*	94.30±12.50**	490.8	<0.001
GGT (U/L)	18.20±9.70	30.40±10.20*	71.71±14.40**	288.5	<0.001
TBA (umol/L)	4.40±2.20	6.50±3.30	13.28±6.10**	21.13	<0.001
TC (mmol/l)	4.20±1.80	5.40±1.60*	5.50±1.50*	9.820	<0.001
TG (mmol/l)	1.80±0.80	2.60±1.00*	3.50±1.80**	16.31	<0.001
LDL-C (mmol/l)	2.90±0.90	3.30±0.70*	3.40±0.80*	5.450	0.005
HDL-C (mmol/l)	1.40±0.40	1.00±0.50*	1.10±0.40*	11.70	<0.001
FPG (mmol/l)	4.31±0.80	6.27±1.11*	7.01±0.90**	135.4	<0.001

\* Compared with the healthy control group,  $P<0.05$ ; # compared with the mild NAFLD group,  $P<0.05$ ; NAFLD – nonalcoholic fatty liver disease; BMI – body mass index; WHR – waist hip ratio; CT – computer tomography; ALT – alanine aminotransferase; AST – aspartate aminotransferase; GGT – gamma-glutamyl transferase; TBA – total bile acid; TC – total cholesterol; TG – triglyceride; LDL-C – low-density lipoprotein cholesterol; HDL-C – high-density lipoprotein cholesterol; FPG – fasting plasma glucose.

moderate-severe NAFLD group (both  $P<0.05$ ). The miR-9 expression levels were also significantly higher in the moderate-severe NAFLD group than that in the mild NAFLD group ( $P<0.05$ ). The relative expression levels of miR-9 were statistically significant in the NASH, non-NASH, and healthy control groups ( $F=156.287$ ,  $P<0.001$ ). Compared with the healthy control group, miR-9 relative expression levels were significantly increased in the NASH and non-NASH groups (both  $P<0.05$ ), and the relative expression levels of miR-9 were also significantly higher in the NASH group than in the non-NASH group ( $P<0.05$ ) (Table 4).

### Cell morphology and proliferation

L-02 cell morphology appeared as fusiform-shaped with transparent cytoplasm. Further, the cells grew robustly and exponential cell growth was observed for 3 days. After 3 days, contact inhibition was observed. The cells reached 80%–90% confluency in 3 days and thus were passaged every 3 days (Figure 1A).

Trypan Blue staining showed 95% viability of L-02 cells at 24 h, 48 h, and 72 h in culture. After induction with oleic acid, steatotic hepatocytes appeared rounded, with blurred edges (Figure 1B). Oleic acid induced steatotic hepatocytes were discarded at the end of the experiments.

### Screening of the optimum concentration of oleic acid and DMSO

Cultured L-02 cells grew normally with very few floating cells seen at oleic acid concentrations of 0 µg/ml (group A), 5 µg/ml (group B), 10 µg/ml (group C), and 20 µg/ml (group D). However, the number of floating cells increased notably when oleic acid concentration was increased to 40 µg/ml (group E). MTT assay was performed to measure cell growth at 24 h, 48 h, and 72 h. The MTT results showed no significant differences between group A, group B, group C, and group D ( $P>0.05$ ), while a significant decrease was observed in group E compared to group A ( $P<0.01$ ) (Table 5 and Figure 2A), indicating that oleic

**Table 3.** General information and biochemical parameters comparison among the healthy control, NASH and non-NASH groups.

	Healthy control group (n=50)	NASH group (n=53)	Non-NASH group (n=52)	F/X2	P
Age (years)	47.26±7.56	46.25±7.2	46.96±8.24	0.239	0.787
Genders (M/F)	32/18	29/24	38/14	3.835	0.147
BMI	22.10±4.40	26.87±4.46*	28.00±4.70*	24.34	<0.001
WHR	0.80±0.30	1.28±0.30*	1.20±0.33*	35.67	<0.001
Liver/spleen CT value	1.33±0.08	0.55±0.29*	0.68±0.29**	150.1	<0.001
Systolic blood pressure (mmHg)	124.2±11.8	125.91±13.06	121.71±13.91	1.789	0.171
Diastolic blood pressure (mmHg)	83.50±6.20	82.70±6.170	83.06±7.13	0.194	0.824
ALT (U/L)	22.40±10.80	69.54±38.48*	55.32±36.25**	30.2	<0.001
AST (U/L)	20.20±10.40	53.59±34.54*	62.07±35.11*	29.03	<0.001
GGT (U/L)	18.20±9.70	55.06±24.31*	42.84±22.24**	45.03	<0.001
TBA (umol/L)	4.40±2.20	9.70±5.26*	9.37±6.39*	18.11	<0.001
TC (mmol/l)	4.20±1.80	5.64±1.55*	5.24±1.54*	10.67	<0.001
TG (mmol/l)	1.80±0.80	2.97±1.25*	3.04±1.69*	14.44	<0.001
LDL-C (mmol/l)	2.90±0.90	3.37±0.69*	3.32±0.80*	5.303	0.006
HDL-C (mmol/l)	1.40±0.40	1.06±0.28*	1.03±0.37*	18.51	<0.001
FPG (mmol/l)	4.31±0.80	6.58±1.06*	6.63±1.11*	88.46	<0.001

\* Compared with the healthy control group,  $P<0.05$ ; # compared with the NASH group,  $P<0.05$ ; NASH – nonalcoholic steatohepatitis; BMI – body mass index; WHR – waist hip ratio; CT – computer tomography; ALT – alanine aminotransferase; AST – aspartate aminotransferase; GGT – gamma-glutamyl transferase; TBA – total bile acid; TC – total cholesterol; TG – triglyceride; LDL-C – low-density lipoprotein cholesterol; HDL-C – high-density lipoprotein cholesterol; FPG – fasting plasma glucose.

**Table 4.** The relative expression of miR-9 in each group.

	Healthy control group (n=50)	Mild NAFLD group (n=58)	Moderate-severe NAFLD group (n=47)	P	NASH group (n=53)	Non-NASH group (n=52)	P
Relative expression of miR-9	5.94±1.21	8.67±0.72	10.55±0.83	<0.05	9.83±1.22	9.18±1.14	<0.05

acid concentrations higher than 20 µg/ml negatively affected cell growth. The oleic acid concentration of 20 µg/ml was determined as the optimal concentration for all subsequent experiments. Various DMSO concentrations tested were: group I (0.0% DMSO), group II (0.1% DMSO), group III (0.2% DMSO), group IV (0.4% DMSO), group V (0.8% DMSO), and group VI (1.6% DMSO). As shown in Table 6 and Figure 2B, no significant difference in cell morphology was observed among the 6 groups ( $P>0.05$ ). Also, DMSO concentrations of less than 1.6% had no influence on cell growth.

### Fluorescent labeling of intracellular lipid droplets by Nile red staining

Under a confocal microscope, L-02 cells in the normal control group showed visible nuclei, clear edges, and rare lipid droplets, as shown in Figure 3. L-02 cells became rounded at 24 h, 48 h, and 72 h after induction with oleic acid. Scattered lipid droplets that stained red with Nile red were observed in the cells. When the lipid droplets were numerous in a single cell, they formed a ring-shape at the edge of the inner membrane. Prolonged induction with oleic acid gradually increased the number of

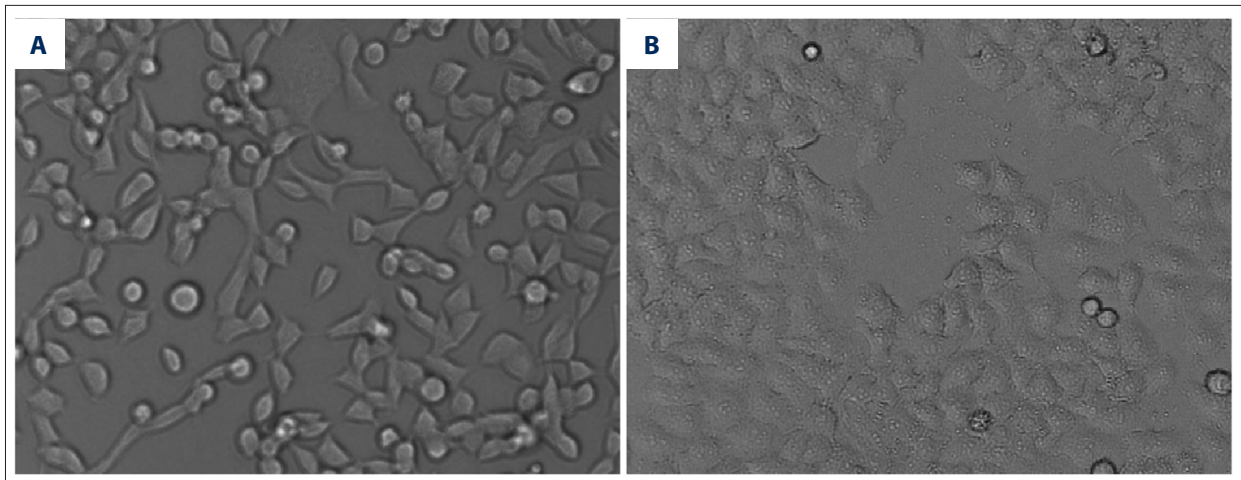


**Figure 1.** Comparison of cell morphology and growth, observed by laser scanning confocal microscopy, of normal L-02 cells and steatotic hepatocytes induced by oleic acid, (A) normal L-02 cells ( $\times 10$ ); (B) steatotic hepatocytes ( $\times 10$ ).

**Table 5.** Comparison of Cell absorbance (OD) by the MTT assay within the oleic acid groups with different concentrations of oleic acid (5 g/ml, 10 g/ml, 20 g/ml and 40 g/ml) at 24 h, 48 h and 72 h, respectively.

	24 h	48 h	72 h	F	P
0 $\mu\text{g/ml}$	0.527 $\pm$ 0.028	0.661 $\pm$ 0.021 <sup>#</sup>	0.926 $\pm$ 0.021 <sup>#@</sup>	742.4	<0.001
5 $\mu\text{g/ml}$	0.543 $\pm$ 0.019	0.658 $\pm$ 0.016 <sup>#</sup>	0.921 $\pm$ 0.018 <sup>#@</sup>	1197.0	<0.001
10 $\mu\text{g/ml}$	0.548 $\pm$ 0.039	0.666 $\pm$ 0.024 <sup>#</sup>	0.925 $\pm$ 0.018 <sup>#@</sup>	460.8	<0.001
20 $\mu\text{g/ml}$	0.547 $\pm$ 0.026	0.652 $\pm$ 0.021 <sup>#</sup>	0.926 $\pm$ 0.009 <sup>#@</sup>	958.9	<0.001
40 $\mu\text{g/ml}$	0.231 $\pm$ 0.021 <sup>*</sup>	0.263 $\pm$ 0.022 <sup>**</sup>	0.306 $\pm$ 0.047 <sup>**@</sup>	13.56	0.0765
F	255.4	714.9	1132		
P	<0.001	<0.001	<0.001		

F – the statistical value of analysis of variance (ANOVA); \* compared to the 0, 5, 10, 20  $\mu\text{g/ml}$ ,  $P < 0.05$ ; # compared to the 24 h,  $P < 0.05$ ; @ compared to the 48 h,  $P < 0.05$ .

intracellular lipid droplets with time (Figure 3A–3D). Figure 3E shows the mean fluorescence intensity of lipid droplets in normal L-02 cells and oleic acid-induced L-02 cells at 24 h, 48 h, and 72 h. Markedly higher mean fluorescence intensities were observed in oleate-induced groups compared to the normal control group (24 h: 863.015 $\pm$ 27.518 vs. 259.756 $\pm$ 28.760; 48 h: 979.825 $\pm$ 50.703 vs. 259.756 $\pm$ 28.760; 72 h: 1154.95 $\pm$ 70.429 vs. 259.756 $\pm$ 28.760; all  $P < 0.05$ ). The fluorescence intensity of the lipid droplets in cells increased with the duration of oleic acid treatment ( $P < 0.05$ ).

#### Intracellular TG content in the cells

As shown in Figure 4A, intracellular TG content increased with the duration of oleic acid induction. As expected, the intracellular TG content in oleate-induced experimental groups at 24 h, 48 h, and 72 h were significantly higher than in the normal control group (24 h: 3.49 $\pm$ 0.13 vs. 1.85 $\pm$ 0.03; 48 h: 4.65 $\pm$ 0.11

vs. 1.81 $\pm$ 0.05; 72 h: 6.63 $\pm$ 0.22 vs. 1.80 $\pm$ 0.03) and the differences were statistically significant (all  $P < 0.01$ , Figure 4B).

#### MiR-9 expression in the fatty liver cells

Changes in miR-9 expression were measured by qRT-PCR analysis in various experimental groups. L02 cells were transfected with miR-9 mimics, mimic control, miR-9 inhibitor, and inhibitor control. MiR-9 expression was significantly increased in the untransfected steatotic cell group, mimic NC group, inhibitor NC group, miR-9 mimic group, and miR-9 inhibitors group, when compared to the NC group (all  $P < 0.05$ ). Further, miR-9 expression in the miR-9 mimic group was significantly higher than in the untransfected steatotic cell group, mimic NC group, and inhibitor NC group, while it was lower in the miR-9 inhibitors group (all  $P < 0.05$ ). No significant differences in miR-9 expression were detected between the untransfected steatotic cell group, mimic NC group, and inhibitor NC group (all  $P < 0.05$ ) (Figure 5).



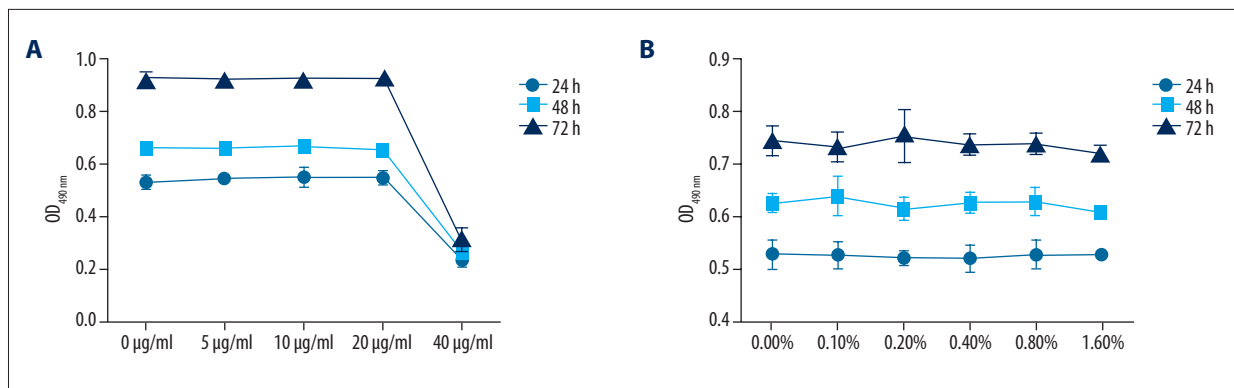


**Figure 2.** Comparison of cell absorbance (OD) by MTT assay in oleic acid groups with different concentrations of oleic acid (5 g/ml, 10 g/ml, 20 g/ml and 40 g/ml) at 24 h, 48 h and 72 h, respectively, (A) Steatotic hepatocytes induced by oleic acid; (B) Steatotic hepatocytes treated with dimethyl sulfoxide (DMSO).

**Table 6.** Effect of dimethyl sulfoxide on L-02 cells by the MTT assay within the dimethyl sulfoxide groups with different concentrations of dimethyl sulfoxide (0.00%, 0.01%, 0.02%, 0.04%, 0.08% and 1.60%).

	24 h	48 h	72 h	F	P
0.00%	0.526±0.028	0.624±0.019 <sup>#</sup>	0.742±0.029 <sup>#@</sup>	176.7	<0.001
0.10%	0.525±0.027	0.637±0.037 <sup>#</sup>	0.730±0.029 <sup>#@</sup>	107.6	<0.001
0.20%	0.519±0.013	0.613±0.022 <sup>#</sup>	0.751±0.051 <sup>#@</sup>	125.5	<0.001
0.40%	0.518±0.025	0.625±0.019 <sup>#</sup>	0.735±0.021 <sup>#@</sup>	247.5	<0.001
0.80%	0.526±0.028	0.626±0.027 <sup>#</sup>	0.735±0.020 <sup>#@</sup>	171.4	<0.001
1.60%	0.525±0.009	0.606±0.008 <sup>#</sup>	0.718±0.013 <sup>#@</sup>	897.4	<0.001
F	0.253	2.105	0.238		
P	0.937	0.079	1.403		

F – the statistical value of analysis of variance (ANOVA); <sup>#</sup> compared to the 24h, *P*<0.05; <sup>@</sup> compared to the 48 h, *P*<0.05.

**Changes of intracellular lipid droplets after transfection**

The accumulation of intracellular lipid droplets is shown in Figure 6A–6F. Visible nuclei, clear edges, and rare lipid droplets were observed in normal L-02 cells. On the other hand, scattered lipid droplets were observed at the edge of the inner membrane in L-02 cells transfected with miR-9 mimics and miR-9 inhibitors. When the lipid droplets were numerous in L-02 cells transfected with miR-9 inhibitors, they were generally located in the perinuclear area. Compared with the NC group (287.76±51.18), the mean fluorescence intensity of the lipid droplets was significantly elevated in the untransfected steatotic cell group, miR-9 mimic group, and miR-9 inhibitor group (all *P*<0.05). Olympus Fluoview ver. 3.0 viewer software tools were used to analyze the mean fluorescence intensity, as shown in Figure 6G. Compared with the untransfected steatotic cell group, the mean fluorescence intensity increased significantly in the miR-9 mimic group (1386.49±43.44 vs. 1022.16±49.65, *P*<0.05), and decreased in the miR-9 inhibitor group (790.92±46.72 vs. 1022.16±49.65, *P*<0.05).

**Prediction and identification of miR-9 target genes**

TargetScan and Pictar databases were used to predict miR-9 target genes. Four genes – Onecut2, SIRT1, REST, and CoREST – were selected for further target validation. Next, the target gene expression levels were measured by qRT-PCR using total RNA purified from tissues and cells of the various experimental groups. Our qRT-PCR results indicated that over-expression of miR-9 was accompanied by down-regulation of Onecut2 and SIRT1, but no changes in REST and CoREST expression levels were detected in the experimental samples (Figure 7A–7D). Western blotting results were consistent with our qRT-PCR results of the expression levels of Onecut2, SIRT1, REST, and CoREST in the NC group, untransfected steatotic cell group, mimic NC group, inhibitor NC group, miR-9 mimic group, and miR-9 inhibitors group (Figure 7E).

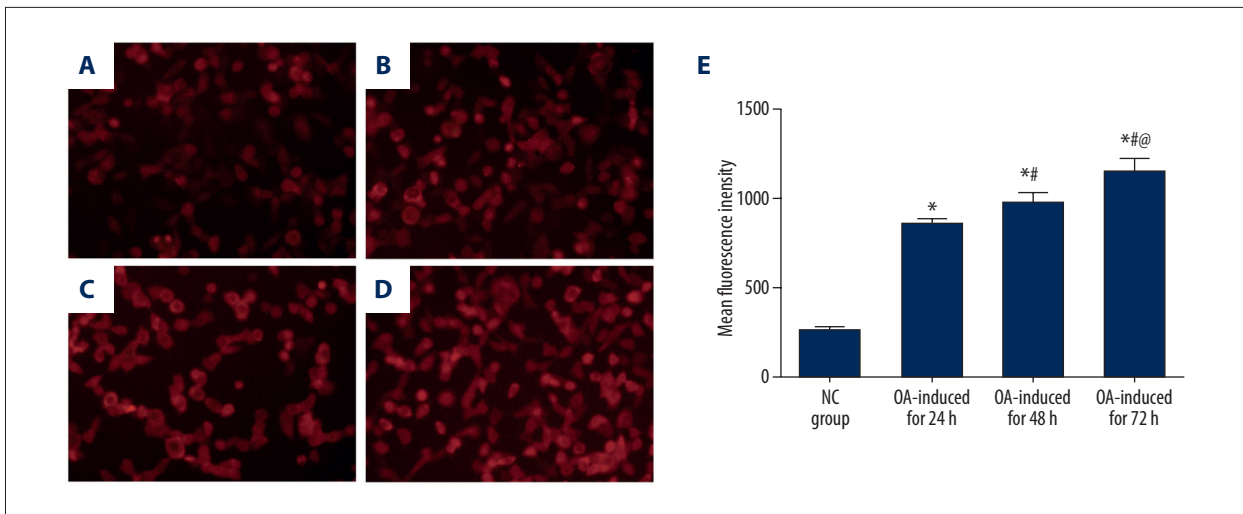


**Figure 3.** Fluorescence-based detection of intracellular lipid droplets by Nile red with laser scanning confocal microscopy (10×40), (A) L-02 cells of normal control group before induction; (B) Steatotic hepatocytes observed at 24 h after induction; (C) Steatotic hepatocytes observed at 48 h after induction; (D) Steatotic hepatocytes observed at 72 h after induction; (E) Changes in lipid droplets in cells. \* Compared to the normal control (NC) group,  $P < 0.05$ ; # Compared to steatotic hepatocytes induced by oleic acid at 24 h,  $P < 0.05$ ; @ Compared to steatotic hepatocytes induced by oleic acid at 48 h,  $P < 0.05$ .

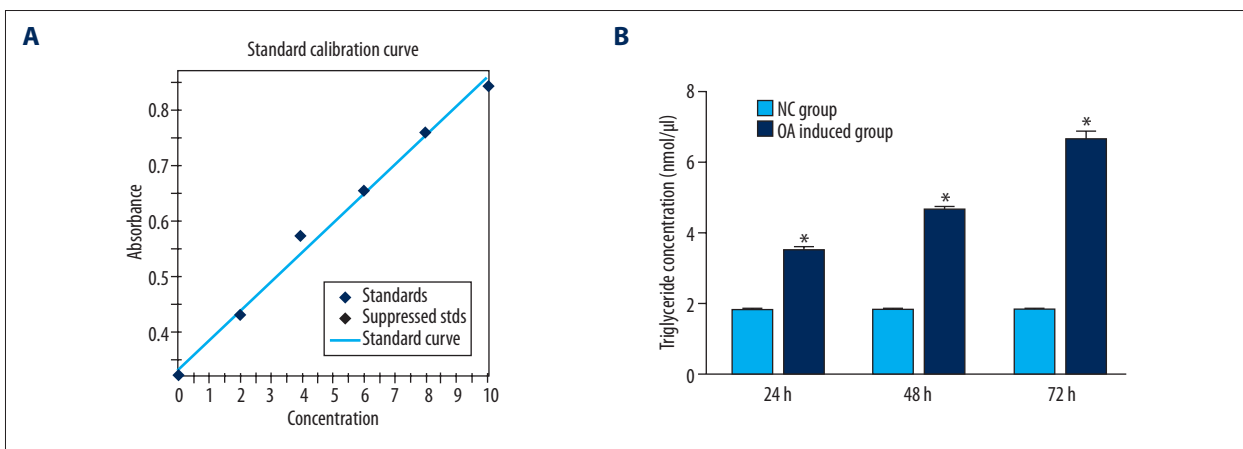


**Figure 4.** The standard curve of triglyceride (TG), revealing the increased intracellular TG content with the longer duration of oleate induction, which was significantly higher than in the normal control group at 24 h, 48 h, and 72 h. (A) Standard curve of TG; (B) Concentration of TG within the steatotic hepatocytes induced by oleic acid at 24 h, 48 h, and 72 h. \* Compared to normal control (NC) group,  $P < 0.05$ .

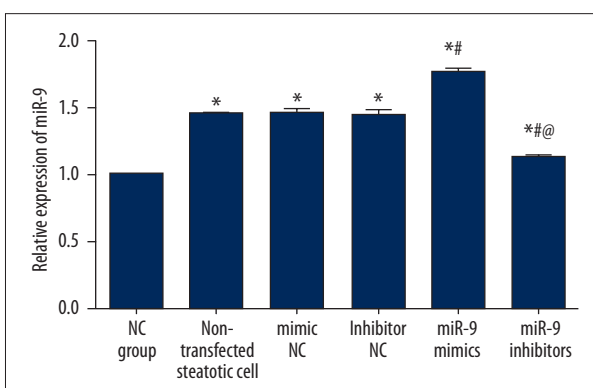


**Figure 5.** Comparison of microRNA-9 expression level between normal L-02 cells and steatotic hepatocytes induced by oleic acid: Changes in microRNA-9 expression after transfection, \* Compared to the normal control (NC) group,  $P < 0.05$ ; # Compared to non-transfected steatotic cell group,  $P < 0.05$ ; @ Compared to the miR-9 mimic group,  $P < 0.05$ .

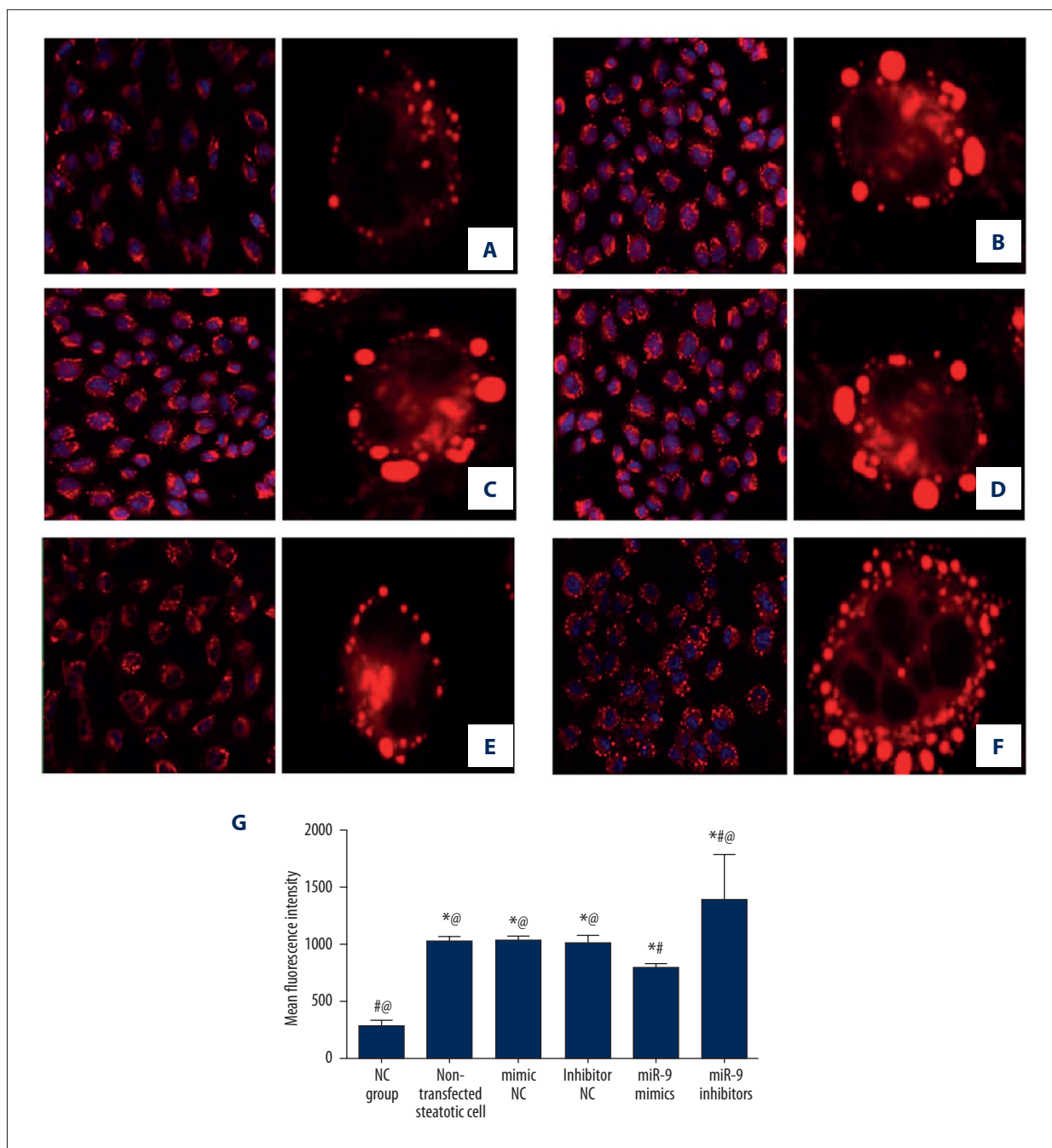


**Figure 6.** The distribution of intracellular lipid droplets in each transfection group observed by laser scanning confocal microscopy (10×40). (A) Normal control (NC) group; (B) Non-transfected steatotic cell group; (C) miR-9 mimic negative control (NC) group; (D) miR-9 inhibitor negative control (NC) group; (E) miR-9 mimic group; (F) miR-9 inhibitor group. (G) The mean fluorescence intensity of lipid droplets in different transfected cells. \* Compared to the normal control (NC) group,  $P < 0.05$ ; # Compared to the non-transfected steatotic cell group,  $P < 0.05$ ; @ Compared to the miR-9 mimic group,  $P < 0.05$ .

**Target relationship between miR-9 and *Onecut2*, *REST*, *SIRT1*, and *CoREST***

Biological predictor targets.org revealed that miR-9 can target to *Onecut2*, *SIRT1*, *REST*, and *CoREST* (Figure 8A). To confirm

that *Onecut2*, *SIRT1*, *REST*, and *CoREST* are direct target genes of miR-9, firstly, the 3'-UTR of *REST* mRNA, 3'-UTR of *CoREST* mRNA, 3'-UTR of *SIRT1* mRNA, and 3'-UTR of *Onecut2* mRNA were inserted to the luciferase reporter gene to obtain luciferase reporter recombinant vector plasmids: pREST-Wt/pREST-Mut,

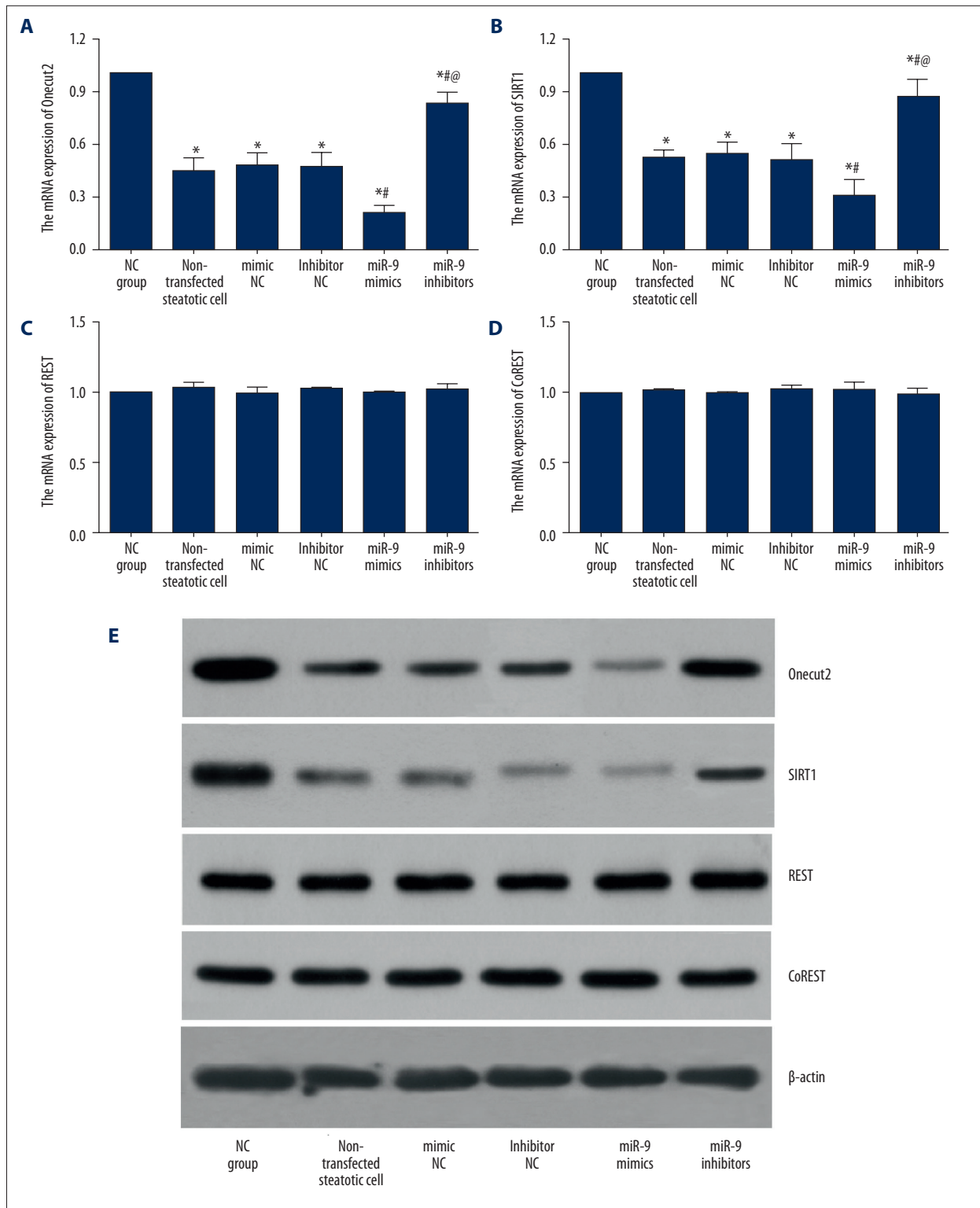


**Figure 7.** Prediction and identification of miR-9 target genes. (A–D) miR-9 target genes expression detection using RT-PCR (A: Onecut2; B: SIRT1; C: REST; D: CoREST). \* Compared to the normal control (NC) group,  $P < 0.05$ ; # Compared to the non-transfected steatotic cell group,  $P < 0.05$ ; @ Compared to the miR-9 mimic group,  $P < 0.05$ . (E) Western blotting to assess the expression of *Onecut2*, *SIRT1*, *REST*, and *CoREST* in the NC group, non-transfected steatotic cell group, mimic NC group, inhibitor NC group, miR-9 mimic group, and miR-9 inhibitors group.

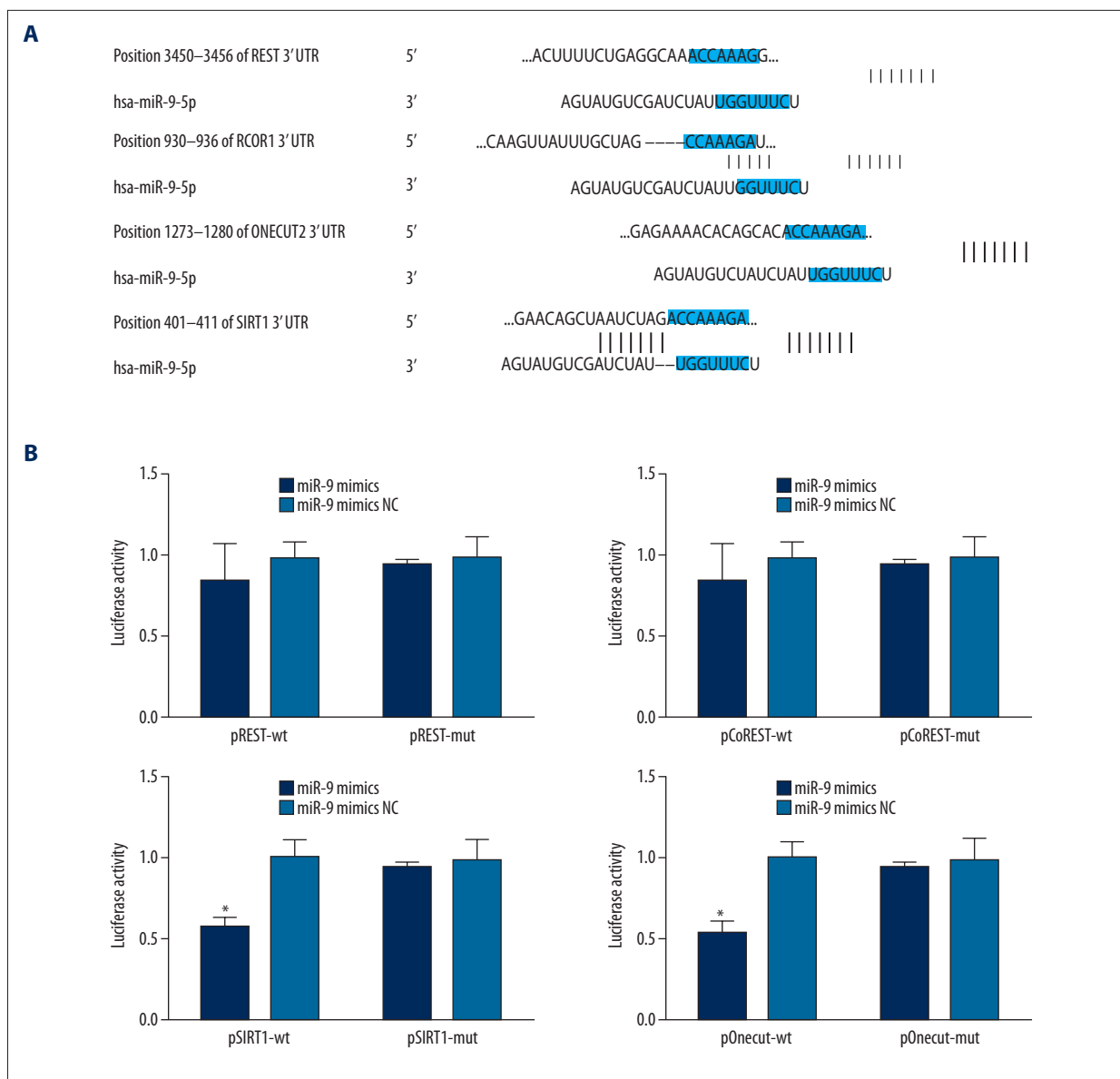


**Figure 8.** (A) Prediction of biological information and the targeting relationships between *SIRT1* and *Onecut2* and miR-9 validated by dual luciferase reporter gene assay. microRNA.org predicts that *Onecut2*, *SIRT1*, *REST*, and *CoREST* are the target genes of miR-9; (B) Dual luciferase reporter gene results assay confirmed that *Onecut2* and *SIRT1* are target genes of miR-9 in L-02 cells (\* Comparison between miR-9 mimic group and miR-9 mimic negative control (NC) group,  $P < 0.05$ ).

pCoREST-Wt/pCoREST-Mut, pSIRT1-Wt/pSIRT1-Mut, and pOne-cut2-Wt/pOnecut2-Mut. Dual luciferase report system results showed that the fluorescence signal of the 3'-UTR of *SIRT1* mRNA and 3'-UTR of the *Onecut2* mRNA co-transfected group decreased by about 42% and 45% compared with the other groups (all  $P < 0.05$ ), but there was no obvious decrease of fluorescence signals in the *REST* group and *CoREST* group (all  $P > 0.05$ ) (Figure 8B). Luciferase signals of the mutant transfected group were not significantly decreased (all  $P > 0.05$ ). Therefore, *Onecut2* and *SIRT1* were potential target genes of miR-9 in L-02 cells, suggesting that miR-9 is able to target *Onecut2* and *SIRT1*.

## Discussion

To investigate prominent miRNA pathways influencing NAFLD, we measured miR-9 expression levels in liver tissues derived from NAFLD patients and performed *in vitro* experiments using normal L-02 cells induced with oleate. The qRT-PCR results from patient tissue samples revealed that miR-9 relative expression levels in mild and moderate-severe NAFLD were strikingly elevated compared to normal healthy controls. Further, miR-9 relative expression levels in moderate-severe NAFLD patients were significantly higher than in mild NAFLD

patients. These results support our hypothesis that miR-9 expression levels are dramatically increased during hepatic steatosis progression and that miR-9 tissue expression levels reflect the disease severity of NAFLD. Previous studies reported that miR-9 expression is highly restricted to brain, liver, and pancreatic islets, and miR-9 plays a pivotal role in exocytosis of insulin [16]. Stimulated exocytosis of insulin is a precisely controlled biological process that has a global impact on body metabolism and on blood glucose levels [29]. An *in vitro* model of oleic acid-induced steatosis was successfully established using normal L-02 liver cells. Results from our detection, characterization, and quantification of intracellular lipid droplet formation and the measurement of TG content in the L-02 cell model showed that oleate induction led to a set of consistent cellular changes that are characteristic of human NAFLD. We used this *in vitro* model to further study NAFLD development in relation to changes in miR-9 levels. Oleic acid is a monosaturated omega-9 FFA that induces hepatic steatosis in HepG2 cells [26]. Oleic acid treatment results in accumulation of intracellular lipid droplets, recapitulating the pathological changes related to early events in the development of liver steatosis [30]. Hepatic steatosis is a typical feature of NAFLD [31] and oleic acid accumulation correlates with widespread cellular apoptosis [32,33], which causes significant tissue damage and triggers adverse tissue responses. For example, overaccumulation of monosaturated fatty acids, like oleate, triggers increased uptake of long-chain saturated fatty acids and leads to cell death due to lipotoxicity. In addition, increased production of reactive oxygen species (ROS) and oxidative stress due to elevated lipid peroxidation further activates apoptotic pathways [34,35].

Fat metabolism in the liver includes oxidation of triglycerides to produce energy, synthesis of lipoproteins, conversion of carbohydrates and proteins into fatty acids and triglycerides, and biosynthesis of cholesterol and phospholipids [36]. Hepatic steatosis is predominantly defined as the accumulation of hepatic lipid, mainly TG, in the liver [37,38]. Tessari et al. defined NAFLD as hepatic TG concentration exceeding 5% of liver weight [39]. In support of this, our measurement of TG levels in patient samples and in L-02 cells revealed a tight relationship between hepatic steatosis and intracellular TG levels. Steatotic hepatocytes exhibited markedly increased lipid content and this increased lipid content worsened with longer duration of oleic acid induction. Consistent with our observations, a previous study reported 2.7 times higher TG content in an FFA-induced steatosis model in L-02 cells compared with controls, indicating the central role for TG in hepatic lipid metabolism and hepatic steatosis [40].

Our study provides strong evidence of significantly increased miR-9 expression level in oleic acid-treated cells, suggesting that miR-9 elevation is associated with NAFLD development.

Abnormal miR-9 expression, due to mutations, deletions, or translocations, has been previously reported and altered expression of miR-9 plays an important role in the development of many diseases [41]. Previous studies showed that miR-9 can function as a novel metastasis suppressor in ovarian cancer, gastric cancer, medulloblastoma, and malignant melanoma tumor [42,43]. Our qRT-PCR data from this study showed significantly increased miR-9 expression levels after experimentally induced hepatic steatosis, but we did not further test whether cell migration pathways were also affected in our experimental set-up, which may have important implications regarding liver cancer progression.

In our study, transient transfection of miR-9 mimics increased miR-9 expression level in oleic acid-induced L-02 cells, as expected, and was accompanied by a significant decrease in intracellular lipid droplets, compared to the normal cells. By contrast, miR-9 expression decreased significantly following transient transfection of miR-9 inhibitors, and intracellular lipid droplets increased significantly in oleate-induced L-02 cells. From these findings, we propose that the biological events underlying the observed accumulation of lipids in our *in vitro* model mirror the NAFLD disease pathogenesis. Thus, based on our results, we conclude that miR-9 levels strongly influence NAFLD development.

Bioinformatics-based prediction, combined with qRT-PCR analysis and Western blotting, identified *Onecut2* and *SIRT1* as the 2 prominent miR-9 target genes under the conditions tested. miRNAs bind to 3'-untranslated regions of target mRNAs and control their expression by either promoting mRNA degradation or inhibiting protein translation [44]. Target identification was, therefore, critical in our study to understand the biological context of the observed effects of miR-9. In this study, *Onecut2* and *SIRT1* were confirmed as miR-9 target genes, which will help future investigations to probe in greater detail the role of miR-9 in NAFLD. Based on the results we obtained in this study, we speculate that miR-9 negatively regulates *Onecut2* and *SIRT1* levels in insulin-secreting cells and both are involved in regulation of insulin secretion, implicating them in NAFLD development [16,45].

## Conclusions

Our present study provides strong evidence that miR-9 level is significantly increased in liver tissues of NAFLD patients and in normal liver cells after experimental hepatic steatosis. While the transient transfection of miR-9 mimics significantly decreased intracellular fat content, transient transfection of miR-9 inhibitors had the opposite effect, as anticipated, and led to significant increases in intracellular fat content. miR-9 was able to target *Onecut2*, *SIRT1*, *REST*, and *CoREST*, but only

*Onecut2* and *SIRT1* in the L-02 cells had a significant response to miR-9 regulation, and miR-9 could significantly down-regulate the expression levels of *Onecut2* and *SIRT1*. Collectively, these results indicate central roles for miR-9 and its target genes, *Onecut2* and *SIRT1*, in the regulation of fat metabolism and in the pathogenesis and development of NAFLD.

## References:

1. Yeh MM, Brunt EM: Pathological features of fatty liver disease. *Gastroenterology*, 2014; 147: 754–64
2. McPherson S, Henderson E, Burt AD et al: Serum immunoglobulin levels predict fibrosis in patients with non-alcoholic fatty liver disease. *J Hepatol*, 2014; 60: 1055–62
3. Utschneider KM, Largajolli A, Bertoldo A et al: Serum ferritin is associated with non-alcoholic fatty liver disease and decreased Beta-cell function in non-diabetic men and women. *J Diabetes Complications*, 2014; 28: 177–84
4. Gruben N, Shiri-Sverdlov R, Koonen DP, Hofker MH: Nonalcoholic fatty liver disease: A main driver of insulin resistance or a dangerous liaison? *Biochim Biophys Acta*, 2014; 1842: 2329–43
5. Kopec AK, Joshi N, Towery KL et al: Thrombin inhibition with dabigatran protects against high-fat diet-induced fatty liver disease in mice. *J Pharmacol Exp Ther*, 2014; 351: 288–97
6. Anderson EL, Howe LD, Fraser A et al: Weight trajectories through infancy and childhood and risk of non-alcoholic fatty liver disease in adolescence: the ALSPAC study. *J Hepatol*, 2014; 61: 626–32
7. Bedossa P, Consortium FP: Utility and appropriateness of the fatty liver inhibition of progression (FLIP) algorithm and steatosis, activity, and fibrosis (SAF) score in the evaluation of biopsies of nonalcoholic fatty liver disease. *Hepatology*, 2014; 60: 565–75
8. Nalbantoglu IL, Brunt EM: Role of liver biopsy in nonalcoholic fatty liver disease. *World J Gastroenterol*, 2014; 20: 9026–37
9. Anstee QM, Day CP: The genetics of NAFLD. *Nat Rev Gastroenterol Hepatol*, 2013; 10: 645–55
10. Estep JM, Goodman Z, Sharma H et al: Adipocytokine expression associated with miRNA regulation and diagnosis of NASH in obese patients with NAFLD. *Liver Int*, 2015; 35: 1367–72
11. Newton KP, Awai HI, Feldstein AE, Schwimmer JB: Letter: gender-associated cell-free microRNA profiles in non-alcoholic fatty liver disease – authors' reply. *Aliment Pharmacol Ther*, 2014; 39: 999
12. Xu P, Mohorianu I, Yang L, Zhao H et al: Small RNA profile in moso bamboo root and leaf obtained by high definition adapters. *PLoS One*, 2014; 9: e103590
13. Farid WR, Verhoeven CJ, de Jonge J et al: The ins and outs of microRNAs as biomarkers in liver disease and transplantation. *Transpl Int*, 2014; 27: 1222–32
14. Lamba V, Ghodke-Puranik Y, Guan W, Lamba JK: Identification of suitable reference genes for hepatic microRNA quantitation. *BMC Res Notes*, 2014; 7: 129
15. Zhao YA, Zhou HL et al: Quantitative study of HCC metastasis related microRNAs in different metastatic potential of hepatocellular carcinoma cell line. *Chinese Journal of liver disease*, 2009
16. Ramachandran D, Roy U, Garg S et al: Sirt1 and mir-9 expression is regulated during glucose-stimulated insulin secretion in pancreatic beta-islets. *FEBS J*, 2011; 278: 1167–74
17. Szabo G, Bala S: MicroRNAs in liver disease. *Nat Rev Gastroenterol Hepatol*, 2013; 10: 542–52
18. Miranda RC, Pietrzykowski AZ, Tang Y et al: MicroRNAs: master regulators of ethanol abuse and toxicity? *Alcohol Clin Exp Res*, 2010; 34: 575–87
19. M PN: World Medical Association publishes the Revised Declaration of Helsinki. *Natl Med J India*, 2014; 27: 56
20. Association. FLAALDSGoCLD. Non-alcoholic fatty liver disease diagnosis and treatment guidelines.. *Chinese Journal of Liver Diseases*, 2006; 14: 161–63
21. Kleiner DE, Brunt EM, Van Natta M et al: Design and validation of a histological scoring system for nonalcoholic fatty liver disease. *Hepatology*, 2005; 41: 1313–21
22. Sanyal AJ, Brunt EM, Kleiner DE et al: Endpoints and clinical trial design for nonalcoholic steatohepatitis. *Hepatology*, 2011; 54: 344–53
23. Nass D, Rosenwald S, Meiri E et al: MiR-92b and miR-9/9\* are specifically expressed in brain primary tumors and can be used to differentiate primary from metastatic brain tumors. *Brain Pathol*, 2009; 19: 375–83
24. Packer AN, Xing Y, Harper SQ, Jones L, Davidson BL: The bifunctional microRNA miR-9/miR-9\* regulates REST and CoREST and is downregulated in Huntington's disease. *J Neurosci*, 2008; 28: 14341–46
25. Chavez-Tapia NC, Rosso N, Tiribelli C: Effect of intracellular lipid accumulation in a new model of non-alcoholic fatty liver disease. *BMC Gastroenterol*, 2012; 12: 20
26. Cui W, Chen SL, Hu KQ: Quantification and mechanisms of oleic acid-induced steatosis in HepG2 cells. *Am J Transl Res*, 2010; 2: 95–104
27. Moellering ER, Benning C: RNA interference silencing of a major lipid droplet protein affects lipid droplet size in *Chlamydomonas reinhardtii*. *Eukaryot Cell*, 2010; 9: 97–106
28. Sun Y, Shen S, Liu X et al: MiR-429 inhibits cells growth and invasion and regulates EMT-related marker genes by targeting *Onecut2* in colorectal carcinoma. *Mol Cell Biochem*, 2014; 390: 19–30
29. Kaihara KA, Dickson LM, Jacobson DA et al: beta-Cell-specific protein kinase A activation enhances the efficiency of glucose control by increasing acute-phase insulin secretion. *Diabetes*, 2013; 62: 1527–36
30. Fujimoto Y, Itabe H, Kinoshita T et al: Involvement of ACSL in local synthesis of neutral lipids in cytoplasmic lipid droplets in human hepatocyte HuH7. *J Lipid Res*, 2007; 48: 1280–92
31. Gomez-Lechon MJ, Donato MT, Martinez-Romero A et al: A human hepatocellular *in vitro* model to investigate steatosis. *Chem Biol Interact*, 2007; 165: 106–16
32. Ricchi M, Odoardi MR, Carulli L et al: Differential effect of oleic and palmitic acid on lipid accumulation and apoptosis in cultured hepatocytes. *J Gastroenterol Hepatol*, 2009; 24: 830–40
33. Zhu Y, Schwarz S, Ahlemeyer B et al: Oleic acid causes apoptosis and dephosphorylates Bad. *Neurochem Int*, 2005; 46: 127–35
34. Wang JW, Wan XY, Zhu HT et al: Lipotoxic effect of p21 on free fatty acid-induced steatosis in L02 cells. *PLoS One*, 2014; 9: e96124
35. Artwohl M, Roden M, Waldhausl W et al: Free fatty acids trigger apoptosis and inhibit cell cycle progression in human vascular endothelial cells. *FASEB J*, 2004; 18: 146–48
36. Wu CH, Lin MC, Wang HC et al: Rutin inhibits oleic acid induced lipid accumulation via reducing lipogenesis and oxidative stress in hepatocarcinoma cells. *J Food Sci*, 2011; 76: T65–72
37. Musso G, Gambino R, Cassader M: Recent insights into hepatic lipid metabolism in non-alcoholic fatty liver disease (NAFLD). *Prog Lipid Res*, 2009; 48: 1–26
38. Johnson NA, Walton DW, Sachinwalla T et al: Noninvasive assessment of hepatic lipid composition: Advancing understanding and management of fatty liver disorders. *Hepatology*, 2008; 47: 1513–23
39. Tessari P, Coracina A, Cosma A, Tiengo A: Hepatic lipid metabolism and non-alcoholic fatty liver disease. *Nutr Metab Cardiovasc Dis*, 2009; 19: 291–302
40. Chu JH, Wang H, Ye Y et al: Inhibitory effect of schisandrin B on free fatty acid-induced steatosis in L-02 cells. *World J Gastroenterol*, 2011; 17: 2379–88

## Acknowledgments

We acknowledge our colleagues for their helpful comments on this paper.

## Competing interests

The authors have declared that no competing interests exist.

41. Xu J, Hu G, Lu M et al: MiR-9 reduces human acyl-coenzyme A: cholesterol acyltransferase-1 to decrease THP-1 macrophage-derived foam cell formation. *Acta Biochim Biophys Sin (Shanghai)*, 2013; 45: 953–62
42. Schraivogel D, Weinmann L, Beier D et al: CAMTA1 is a novel tumour suppressor regulated by miR-9/9\* in glioblastoma stem cells. *EMBO J*, 2011; 30: 4309–22
43. Rotkrue P, Akiyama Y, Hashimoto Y et al: MiR-9 downregulates CDX2 expression in gastric cancer cells. *Int J Cancer*, 2011; 129: 2611–20
44. Gennarino VA, D'Angelo G, Dharmalingam G et al: Identification of microRNA-regulated gene networks by expression analysis of target genes. *Genome Res*, 2012; 22: 1163–72
45. Joglekar MV, Parekh VS, Hardikar AA: Islet-specific microRNAs in pancreas development, regeneration and diabetes. *Indian J Exp Biol*, 2011; 49: 401–8